Seismic passive resistance of cantilever retaining wall with an efficient adaptive failure mechanism

G. Santhoshkumar[1] and P. Ghosh[1]

[1] Department of Civil Engineering, Indian Institute of Technology Kanpur, Kanpur – 208016, India.

ABSTRACT

This technical paper emphasizes on the automatic generation of the failure surface to determine the passive resistance of a non-vertical cantilever retaining wall with a cohesionless backfill subjected to the earthquake loading. The present study utilises the efficiency of the method of stress characteristics along with the recently proposed modified pseudo-dynamic approach. Unlike the available literature reporting a predetermined failure surface, the present study is capable to evolve the failure surface automatically in the course of analysis. The efficacy of the proposed method in obtaining the least passive resistance is critically discussed here along with the effect of various parameters such as soil friction angle, damping ratio, wall geometry, wall roughness, and predominant shear and primary wave propagation.

Keywords: earth pressure; passive resistance; retaining walls; seismic waves; stress characteristics

1 INTRODUCTION

Determination of earth pressure has been the subject of interest among the major part of the research fraternity as it develops the basis for dealing with several geotechnical problems. Mononobe and Okabe (1929) proposed the most simplified theory to include the effect of seismicity into the classical Coulomb's earth pressure theory and named it as the pseudo-static method. This method is still widely used by the practising engineers due to its simplicity and conservativeness. The method adopts uniform soil acceleration throughout the height of the retaining wall. To subdue the limitation, Steedman and Zeng (1990) proposed the original pseudo-dynamic approach, which was later improved by Choudhury and Nimbalkar (2005). The pseudo-dynamic approach includes the phase effect of the primary and shear waves along with the ground amplification of dry elastic backfill. Later on, various researchers solved many useful geotechnical problems using this theory (Ghosh, 2007; Basha and Babu, 2009). Later, Bellezza, (2015) and Pain et al. (2017) proposed a viscoelastic soil model to address the damping effect in the original pseudo-dynamic method along with the stress free ground surface. However, in almost all the cases, a definite failure surface was assumed before the analysis, which might not be the true one especially under the passive state. Sokolovski (1960) had successfully implemented the method of stress characteristics to trace the path of the failure mechanism in soil under the static condition. Later, several researchers explored the possibility of inclusion of seismicity in the method using the available pseudo-static and original pseudo-dynamic approach (Kumar and Chitikela, 2002; Santhoshkumar and Ghosh, 2018). In the present study, the feasibility of using the modified pseudo-dynamic method along with the method of stress characteristics has been investigated to obtain the critical passive pressure coefficients. Besides the actual non-linear failure surface generated automatically, the present method is capable of providing the stress contours developed in the influence domain as well.

2 PROBLEM DEFINITION

Under the passive condition, a rigid non-vertical cantilever retaining wall inclined at an angle (β) supports a cohesionless backfill with internal friction angle (ϕ) and soil-wall interface friction (δ) over the height (H) (Fig. 1).

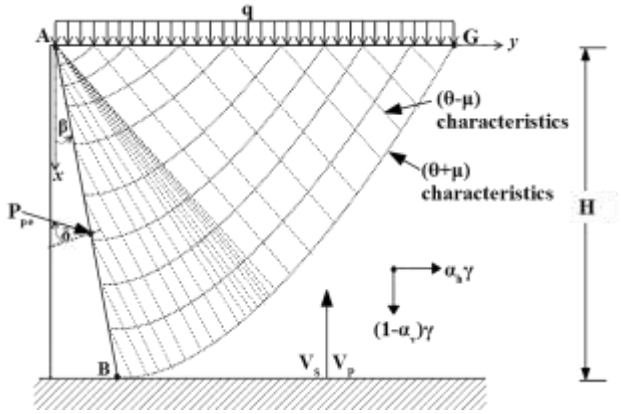

Fig.1. Problem definition

Under the seismic condition, the standing shear and primary waves get propagated through the viscoelastic soil domain with a velocity V_s and V_p, respectively. Under the harmonic base excitation with base

accelerations $k_h g$ and $k_v g$, the seismic accelerations at any depth x can be expressed as a_h and a_v as given in Eq. (1) (Bellezza, 2015; Pain et al., 2017).

$$a_h(x,t)=\frac{k_h g}{C_s^2+S_s^2}\left\{\begin{matrix}(C_sC_{sx}+S_sS_{sx})\cos(\omega_s t)+\\(S_sC_{sx}-C_sS_{sx})\sin(\omega_s t)\end{matrix}\right\} \quad (1a)$$

$$a_v(x,t)=\frac{k_v g}{C_p^2+S_p^2}\left\{\begin{matrix}(C_pC_{px}+S_pS_{px})\cos(\omega_p t)+\\(S_pC_{px}-C_pS_{px})\sin(\omega_p t)\end{matrix}\right\} \quad (1b)$$

where,

$$C_{sx}=\cos\left(\frac{y_{s1}x}{H}\right)\cosh\left(\frac{y_{s2}x}{H}\right);C_s=C_{sx}(H);$$

$$S_{sx}=-\sin\left(\frac{y_{s1}x}{H}\right)\sinh\left(\frac{y_{s2}x}{H}\right);S_s=S_{sx}(H);$$

$$C_{px}=\cos\left(\frac{y_{p1}x}{H}\right)\cosh\left(\frac{y_{p2}x}{H}\right);C_p=C_{px}(H);$$

$$S_{px}=-\sin\left(\frac{y_{p1}x}{H}\right)\sinh\left(\frac{y_{p2}x}{H}\right);S_p=S_{px}(H);$$

$$y_{s1}=\frac{\omega H}{V_s}\sqrt{\frac{\sqrt{1+4D^2}+1}{2\left(1+4D^2\right)}};y_{s2}=-\frac{\omega H}{V_s}\sqrt{\frac{\sqrt{1+4D^2}-1}{2\left(1+4D^2\right)}};$$

$$y_{p1}=\frac{\omega H}{V_p}\sqrt{\frac{\sqrt{1+4D^2}+1}{2\left(1+4D^2\right)}};y_{p2}=-\frac{\omega H}{V_p}\sqrt{\frac{\sqrt{1+4D^2}-1}{2\left(1+4D^2\right)}};$$

3 ANALYSIS

3.1 Method of characteristics

The method was more elaborately discussed by Sokolovski (1960). Taking origin of the x-y coordinate system at the top of the retaining wall as shown in Fig. 1, two families of characteristic curves can be obtained which should satisfy the following Eqs. (2) and (3) along (θ-μ) and (θ+μ) characteristic, respectively.

$$\frac{dy}{dx}=\tan(\theta-\mu);\frac{d\eta}{dx}=\frac{X\sin(\theta+\mu)-Y\cos(\theta+\mu)}{2\sigma\sin\phi\cos(\theta-\mu)}; \quad (2)$$

$$\frac{dy}{dx}=\tan(\theta-\mu);\frac{d\xi}{dx}=-\frac{X\sin(\theta-\mu)-Y\cos(\theta-\mu)}{2\sigma\sin\phi\cos(\theta+\mu)}; \quad (3)$$

where, X and Y are body forces along x- and y-direction, σ is the distance on the Mohr stress diagram, between the centre of the Mohr circle and a point where the Coulomb's linear failure envelope intersects the σ-axis.

$$\left.\begin{matrix}\eta\\\xi\end{matrix}\right\}=\left[\left(\frac{\cot\phi}{2}\ln\frac{\sigma}{\sigma_0}\right)\mp\theta\right];\mu=\left(\frac{\pi}{4}-\frac{\phi}{2}\right);$$

The orientation of the major principal stress (θ) and the different types of stress fields are detailed in Santhoshkumar and Ghosh (2018) and Kumar and Chitikela (2002).

3.2 Seismic passive pressure coefficient

A finite amount of surcharge is always needed to avoid the floating error (Santhoshkumar and Ghosh, 2018). However, the effect of surcharge can be removed using the principle of superposition. The seismic passive earth pressure coefficient can therefore be expressed as

$$K_{p\gamma}=\frac{(P_{pe}-K_{pq}qH)}{0.5\gamma H^2} \quad (4)$$

where, the magnitude of K_{pq} can be obtained from the closed form equations proposed by Santhoshkumar and Ghosh (2018).

4 RESULTS AND DISCUSSION

The computations have been performed for a range of input parameters: γ = 18 kN/m^3, $q = 0.01\gamma H$, ϕ = 30° – 40°, $\delta = 0 - \phi$, β = -10° – +10°, D = 5% – 20%, $\omega H/V_s$ = 0.94, 1.87, V_p/V_s = 1.87. k_h = 0 – 0.3, $|k_v|$ = 0 – k_h

4.1 Effect of k_h and k_v

Unlike the usual pseudo-static and original pseudo-dynamic method, the modified pseudo-dynamic method considers complex mathematical equations for the seismic accelerations (Eq. 1). For $\omega H/V_s$ = 0.94 and $\omega H/V_p$ = 0.50, both the horizontal and the vertical acceleration simultaneously attain their respective peak value when $k_h > 0$ and $k_v > 0$. However, for $\omega H/V_s$ = 1.87 and $\omega H/V_p$ = 1, the accelerations reach their peak when $k_h > 0$ and $k_v < 0$. This clearly demonstrates that the critical combination of k_h and k_v is a frequency dependent phenomenon in this method. Table 1 shows the effect of k_v on $K_{p\gamma}$ with different frequency ratios.

Table 1. Variation of $K_{p\gamma}$ for different $\omega H/V_s$ ratios with ϕ = 40°, $\delta = 2\phi/3$ and D = 10%.

Frequency ratio	k_h	k_v = -0.5k_h	k_v = 0	k_v = 0.5k_h
$\omega H/V_s$ = 0.94, $\omega H/V_P$ = 0.5	0.0	12.23	12.23	12.23
	0.1	11.88	11.20	10.51
	0.2	11.43	10.051	8.679
$\omega H/V_s$ = 1.87, $\omega H/V_P$ = 1.0	0.0	12.233	12.23	12.23
	0.1	9.97	10.79	11.22
	0.2	7.274	9.02	10.07

Fig. 2 shows the distribution of normalized stress along the height of the wall with different k_v values. It can be observed that the system attains the lesser passive resistance when $k_v < 0$ for the given input parameters. It is worth noting that for the case of $\omega H/V_s$ = 1.87 and $\omega H/V_p$ = 1, both the shear and the primary waves are closer to the fundamental frequency (π/2). Hence, the present study is carried out in this frequency range.

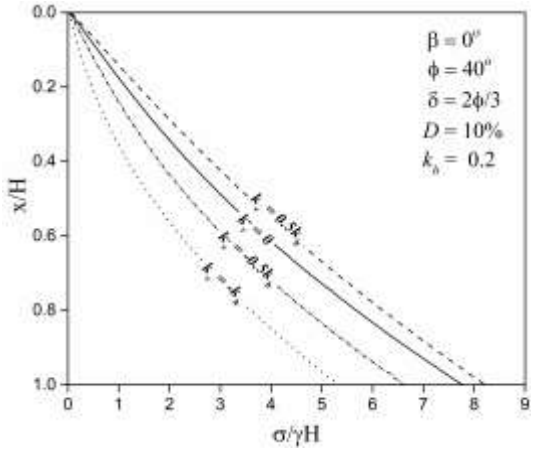

Fig. 2. Normalized stress distribution for different values of k_v with $\omega H/V_s$ = 1.87, $\omega H/V_p$ = 1.0 and D = 10%.

4.2 Effect of soil friction and wall inclination

Fig. 3 presents the variation of $K_{p\gamma}$ with k_h for different soil friction angles (ϕ) and wall inclinations (β).

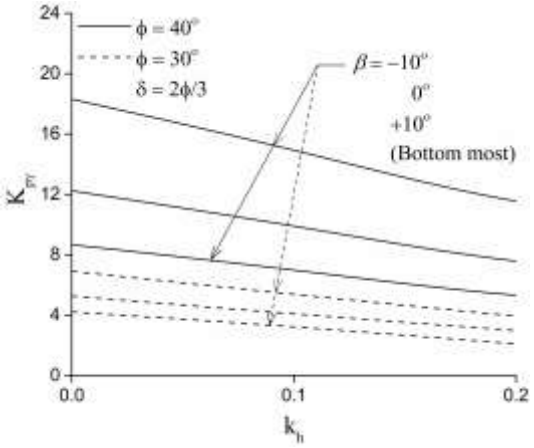

Fig. 3. Variation of $K_{p\gamma}$ for different β and ϕ with k_v = -0.5k_h, $\omega H/V_s$ = 1.87, $\omega H/V_p$ = 1.0 and D = 10%.

From Table 1 and Fig. 3, it can be observed that the magnitude of $K_{p\gamma}$ continuously decreases with the increase in k_h and β irrespective of the frequency ratio adopted. However, the frequency ratio should be chosen in such a way that it should be close to the fundamental frequency (π/2) for the effective inclusion of soil damping.

4.3 Effect of wall roughness and soil damping

Fig. 4 shows the normalized stress distribution for different δ. In addition to the magnitude of the seismic passive pressure, the nature of stress distribution is also greatly affected by the wall roughness (Fig. 4). Damping ratio is found to be a dominant factor when the seismic waves are closer to their fundamental frequency. Hence the normalized stress distribution for different D are reported in Fig. 5. It can be seen that the passive pressure decreases with decrease in the damping ratio.

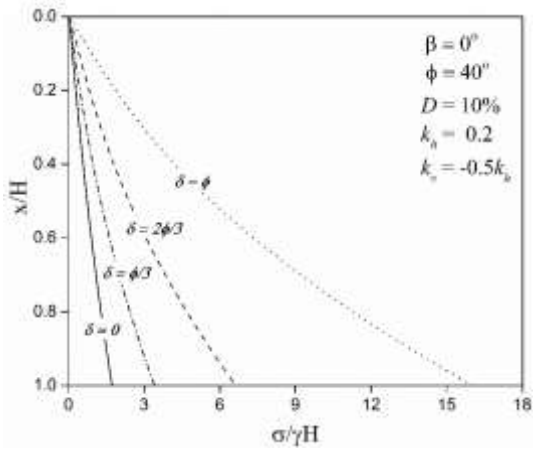

Fig. 4. Normalized stress distribution for different values of δ.

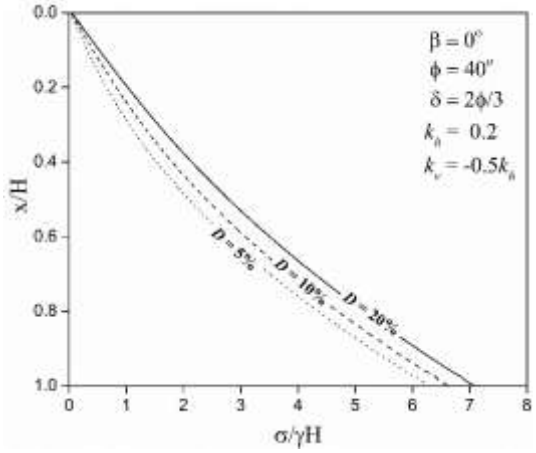

Fig. 5. Normalized stress distribution for different values of D.

4.4 Failure surface and stress contours

No predefined failure surface is assumed in the analysis rather it has been generated automatically during the analysis as shown in Fig. 6. The non-linearity of the failure surface increases with increase in the seismicity.

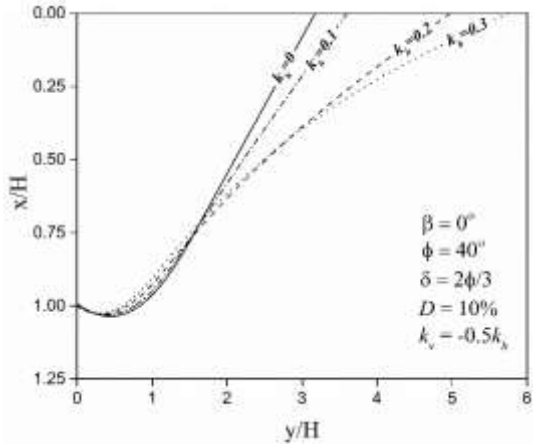

Fig. 6. Non-linear failure surfaces with increasing seismic acceleration for $\omega H/V_s$ = 1.87 and $\omega H/V_p$ = 1.0.

The normalized stress contour in Fig. 7 confirms that the passive pressure gradually increases with the depth from the ground surface and decreases with increase in

the seismic acceleration.

5 COMPARISON

In Table 2, the magnitudes of $K_{p\gamma}$ obtained from the present analysis are compared with the values available in the literature. The present values are found to be the least compared to the values reported in the literature.

Table 2. Comparison of $K_{p\gamma}$ for $\phi = 30^o$, $\beta = 0^o$, $\delta = \phi$, $k_v = 0$, $\omega H/V_s = 0.94$ and $D = 10\%$.

Available studies	$k_h = 0$	$k_h = 0.1$	$k_h = 0.2$
Soubra (2000)	6.860	6.350	5.790
Kumar and Chitikela (2002)	6.563	6.083	5.562
Rao and Choudhury (2005)	6.678	6.235	5.889
Shukla (2014)	10.095	9.017	7.891
Tang et. al (2014)	6.450	6.000	5.500
Pain et. al (2017)	6.671	5.948	5.104
Santhoshkumar and Ghosh (2018)	6.559	6.097	5.595
Present analysis	6.559	5.864	5.011

6 CONCLUSIONS

Using the method of stress characteristics coupled with the modified pseudo-dynamic approach, the seismic passive resistance of a non-vertical cantilever retaining wall is obtained without assuming any preset failure mechanism. The effect of various parameters such as soil friction angle, wall roughness and inclination, soil damping and phase difference of the seismic waves on the passive resistance is explored. The non-linear stress distribution and the failure surface are also presented along with the stress contours. The present method is found to provide the least passive resistance among the available studies in the literature. Thus, it can be directly adopted in the seismic analysis of the retaining wall under the passive condition.

REFERENCES

Basha, B. M., & Babu, G. L. S. (2009). Computation of sliding displacements of bridge abutments by pseudo-dynamic method. *Soil Dynamics and Earthquake Engineering*, *29*(1), 103–120.

Bellezza, I. (2015). Seismic active earth pressure on walls using a new pseudo-dynamic approach. *Geotechnical and Geological Engineering*, *33*(4), 795–812.

Choudhury, D., & Nimbalkar, S. (2005). Seismic passive resistance by pseudo-dynamic method. *Géotechnique*, *55*(9), 699–702.

Ghosh, P. (2007). Seismic passive earth pressure behind non-vertical retaining wall using pseudo-dynamic analysis. *Geotechnical and Geological Engineering*, *25*(6), 693–703.

Kumar, J., & Chitikela, S. (2002). Seismic passive earth pressure coefficients using the method of characteristics. *Canadian Geotechnical Journal*, *39*(2), 463–471.

Mononobe, N., & Matsuo, H. (1929). On the determination of earth pressure during earthquake. In *Proceedings of the World Engineering Conference*, 177–185.

Okabe, S. (1926). General theory of earth pressure. *Journal Japan Society of Civil Engineering*, *12*(1), 311.

Pain, A., Choudhury, D., & Bhattacharyya, S. K. (2017). Seismic passive earth resistance using modified pseudo-dynamic method. *Earthq Eng. and Eng. Vibration*, *16*(2), 263–274.

Santhoshkumar, G., & Ghosh, P. (2018). Seismic passive earth pressure on an inclined cantilever retaining wall using method of stress characteristics – A new approach. *Soil Dynamics and Earthquake Engineering*, *107*(1), 77–82.

Shukla, S. K. (2014). Seismic passive earth pressure from the sloping c-ϕ soil backfills. *Indian Geotechnical Journal*, *44*(1), 107–111.

Sokolovski, V. V. (1960). *Statics of Soil Media* (2nd ed.). London: Butterworths Scientific Publications.

Soubra, A.H. (2000). Static and seismic passive earth pressure coefficients on rigid retaining structures. *Canadian Geotechnical Journal*, *37*(2), 463–478.

Steedman, R. S., & Zeng, X. (1990). The influence of phase on the calculation of pseudo-static earth pressure on a retaining wall. *Géotechnique*, *40*(1), 103–112.

Subba Rao, K. S., & Choudhury, D. (2005). Seismic passive earth pressures in soils. *Journal of Geotechnical and Geoenvironmental Engineering*, *131*(1), 131–135.

Tang, C., Phoon, K.-K., & Toh, K.-C. (2014). Lower-bound limit analysis of seismic passive earth pressure on rigid walls. *International Journal of Geomechanics*, 14(5), 04014022.

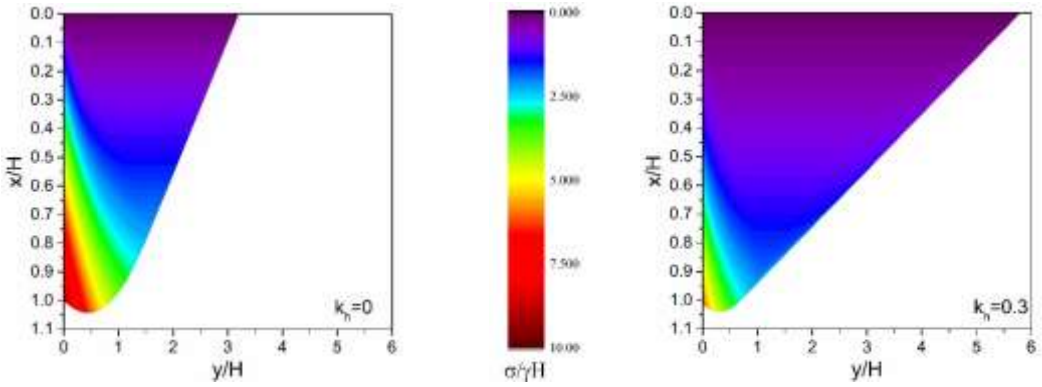

(a) static **(b) Dynamic**

Fig. 7. Normalized stress contours for $\beta = 0°$, $\phi = 40°$, $\delta = 2\phi/3$, $k_v = -0.5k_h$, $\omega H/V_s = 1.87$, $\omega H/V_p = 1.0$ and $D = 10\%$.